Effect of Welding Parameters and H_2S Partial Pressure on the Susceptibility of Welded HSLA Steels to Sulfide Stress Cracking

A standard controlling usage of welded high-strength, low-alloy steels in sour enviroments is assessed

BY G. M. OMWEG, G. S. FRANKEL, W. A. BRUCE, J. E. RAMIREZ, AND G. KOCH

ABSTRACT. The susceptibility of welded API 5L X70 and X80 steels to sulfide stress cracking (SSC) was investigated using two applied stresses and three H_2S concentrations. The effect of peak weld hardness was examined by using three welding conditions. Weld hardness was characterized with Rockwell C and Vickers (HV) 10-kg hardness mapping. Hardness mapping revealed the inadequacy of Rockwell C hardness (HRC) measurements, which is specified by the National Association of Corrosion Engineers (NACE) MR0175 standard, for testing narrow heat-affected zone (HAZ) regions because of the size of the indenter. Several welds meeting the HRC 22 requirement failed by SSC. Several weld conditions containing hardness exceeding 248 HV, which is equivalent to HRC 22, were resistant to SSC at low H_2S concentrations, suggesting that cap hardness levels exceeding 248 HV are suitable for sour service. Hardness level dictated the performance of the X70 material, while the X80 was more susceptible at lower hardness due to localized plastic deformation in intercritically reheated HAZ regions. The centerline segregation region (CSR) in the X70 material was exposed to the corrosive environment at the sample surface as an artifact of the sample preparation, and played an important role in the susceptibility to both SSC and hydrogen-induced cracking (HIC).

Introduction

The hardness of carbon steels currently determines their fitness for sour (aqueous and H_2S-containing) environments according to National Association of Corrosion Engineers (NACE) MR0175, which requires that carbon steel and its weldments not exceed a Rockwell C hardness (HRC) of 22 for these applications (Ref. 1). Steels exceeding the HRC 22 threshold are more susceptible to sulfide stress cracking (SSC), a form of hydrogen embrittlement (HE) (Refs. 2–4). The suitable sour service materials listed by NACE MR0175 are based on their resistance to SSC either in actual field applications or in laboratory testing using the NACE TM0177 test method, which is a severe, accelerated exposure test (Ref. 5). The HRC 22 hardness requirement precludes the use of many high-strength low-alloy (HSLA) steels, especially in the as-welded condition, due to either high base material hardness or to the formation of localized high-hardness regions in the weld heat-affected zone (HAZ). HAZ regions have shown heightened susceptibility to SSC in both service and laboratory environments (Ref. 3). The NACE MR0175 requirement may be overly conservative for HSLA steels due to their low carbon contents and high toughness.

The oil and gas industries have increasing need for the use of HSLA steels due to the cost savings they afford, especially in long piping systems that transport crude oil or natural gas. Transport conditions, however, are becoming increasingly sour (higher H_2S concentrations) and the use of higher strength HSLA grades is prevented where NACE MR0175 is employed as a governmental regulation. Of particular importance is the performance of pipeline girth welds used to connect pipe segments in the field. Circumferential girth welds are typically multipass welds, in which subsequent welds temper underlying hard HAZ regions, leaving the hardest HAZ regions in the final untempered cap passes. The cap passes are on the exterior of the pipeline girth weld and thus are exposed to lower hydrogen concentrations than weld regions in contact with the sour environment within the pipe. Because SSC is a HE mechanism, higher hardness values (exceeding HRC 22) should be tolerable in hard weld cap regions, which are exposed to relatively low hydrogen concentrations. Testing performed at TWI showed that, in fact, hard external weld regions exceeding a Vickers hardness (HV) of 300 (248 HV = HRC 22) were resistant to SSC in a stressed pipe containing the NACE test solution (Ref. 6). This investigation was aimed at assessing the conservatism of the NACE requirements for HSLA weldments, with focus on weld hardness requirements and extrapolation to service conditions. Many of the corrosion and embrittlement aspects of this work are described elsewhere (Refs. 7, 8).

KEYWORDS

Corrosion
High-Strength Steels
Piping/Tubing
GMAW
Sour Environment
Sulfide Stress Cracking

Experimental

The materials investigated were API 5L X70 and X80 spiral-welded high-strength low-alloy (HSLA) line pipe materials. Table 1 lists the steel compositions, the values of carbon equivalent CE (IIW), cracking parameter, P_{cm}, and the pertinent pipe dimensions, including outer diameter (OD) and wall thickness (t). The X80 was very low in carbon, just above saturation in ferrite (0.022 wt-% C). Both alloys are low-sulfur steels (Ref. 9). The primary carbo-nitride-forming elements in the X70 and X80 are vanadium and niobium, respectively. The P_{cm} values are more relevant measures of the hardenability of these alloys than the CE values. The X70 has a higher susceptibility to hydrogen cracking (higher P_{cm} value), pri-

G. M. OMWEG and G. S. FRANKEL are with Fontana Corrosion Center, The Ohio State University, Columbus, Ohio. W. A. BRUCE and J. E. RAMIREZ are with Edison Welding Institute, Columbus, Ohio. G. KOCH is with CC Technologies, Inc., Dublin, Ohio.

Table 1 — API 5L Steel Pipeline Base Alloy Compositions (wt-%) and Pipe Dimensions

	Alloy	
	X70	X80
C	0.16	0.029
Mn	1.6	1.86
P	0.013	0.008
S	<0.003	0.003
Si	0.32	0.35
Ni	<0.01	0.11
Cr	0.02	0.06
Mo	<0.01	0.25
Cu	0.01	0.22
V	0.08	<0.005
Al	0.03	0.03
Ti	0.01	0.02
Nb	0.04	0.10
CE	0.47	0.45
P_{cm}	0.26	0.170
OD	34.75 in.	42 in.
t	0.75 in.	0.55 in.

marily due to its much higher carbon content. The X70 would be expected to form harder coarse-grain heat-affected zone (CGHAZ) transformation products.

The as-received microstructure of the X70 pipe steel consisted of banded, fine-grained ferrite + pearlite as shown by the long transverse section in Fig. 1A. The X70 contained a heavily banded centerline segregation region (CSR) characterized by thicker, more continuous banding, as shown in Fig. 1B. This region is compositionally different due to segregation of elements like C and Mn (Ref. 10). As a result, the alloy-rich bands are more hardenable than the alloy-lean bands. In contrast, the X80 did not contain large amounts of carbide, a banded microstructure, or a visible CSR. Figure 2 reveals fine-grained ferrite, large secondary ferrite grains, and granular bainite in the X80 base material. The observed differences in microstructure between X70 and X80 steel pipes result from different chemical composition and steel processing routes.

Metallographic sections were taken in two orientations relative to the pipe axis: longitudinal (L) and longitudinal-transverse (LT). The through-wall hardness profile of each pipeline steel was measured using the Rockwell C and Vickers 10-kg hardness test methods, as shown schematically in Fig. 3.

Girth welds were simulated using a seam weld geometry due to the difficulty foreseen in performing actual girth welds on large pipe sections without the proper automated gas metal arc welding (GMAW) equipment. Two 6 in. × 24 in. unflattened plates cut from the pipe stock were utilized for each joint. The plates were tack welded to a 2-in.-thick steel plate to provide the necessary constraint during cooling. A small carbon steel ⅜ in. × 1 in. backing bar was incorporated into the joint to facilitate the deposition of the root passes. The mock-up weld geometry appears in Fig. 4. The joint geometry was chosen to duplicate a typical GMAW girth weld joint: a 0.25-in. root opening with a 12-deg included angle. All root passes were deposited using low arc energy (15.1 kJ/in.) and the weld interpass temperature was measured using a contact thermocouple. The subsequent fill passes created the gauge material isolated in the tensile specimens for SSC testing. The fill pass weld preheat and input energy were varied to achieve three desired ranges in specimen peak hardness for each pipe steel. These parameters were chosen based on the results of preliminary weld trials. The parameters used for the fill passes in each weld condition appear in Table 2. Condition I, II, and III welds correspond to hard, medium, and soft gauge regions, respectively, in the final simulated girth welds.

The weld cap passes were all performed utilizing the low heat input and a room temperature (RT) preheat in order to minimize tempering effects, thus improving the predictability of the peak hardness from preliminary bead-on-plate weld data. Low heat input weld cap passes were omitted from the Condition III welds for both base materials in order to prevent localized hard spots in these soft weld conditions. The welds were performed at Edison Welding Institute (EWI) using an automated GMAW station, which allowed for accurate control of the weld travel speed. Each weld pass was visually inspected for undercutting, incomplete fusion, and slag. The pertinent welding process conditions common to all welds (both X70 and X80) appear in Table 3. The typical composition for the ER70S-3 filler wire is 0.08% C, 1.1% Mn, and 0.6% Si. The joined material was milled flat on the upper and lower surfaces and screened for defects using X-ray radiography. Transverse weld tensile specimens were machined in accordance with the specifications in NACE TM0177-A — Fig. 4. The machined tensile specimens contained a weld centered in the gauge length.

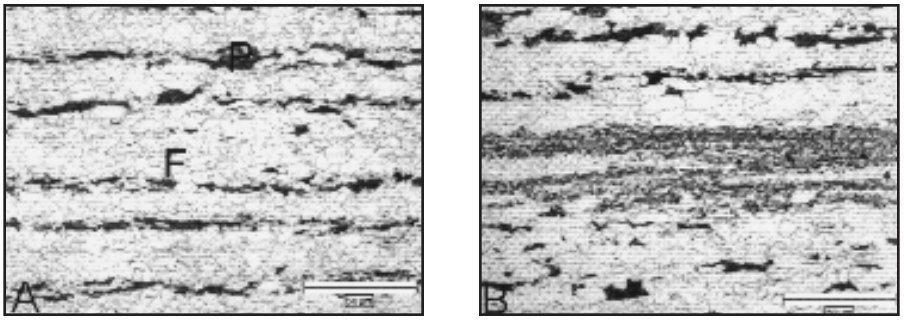

Fig. 1 — X70 long transverse section, 2% Nital etch. A — Fine-grained ferrite; B — centerline segregation region. F=ferrite; P=pearlite.

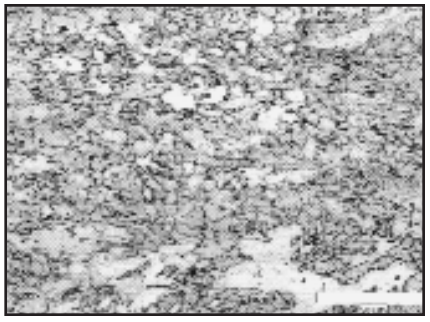

Fig. 2 — X80 LT section, 2% Nital etch.

In order to systematically quantify both the peak weld hardness and hardness distribution in each tensile sample, weld hardness mapping was performed. Metallographic sections were isolated from each weld condition. These sections were taken from regions of the milled weld plates that were adjacent to the material machined for the NACE TM0177-A samples. Each weld was mounted, polished, and etched with 2% Nital. The approximate weld centerline was then scribed across the etched surface as it provided a reference point for the hardness mapping grid and also aided sample alignment on the hardness testing stage. Hardness mapping was performed using both a Rockwell C indenter and a Vickers 10-kg indenter — Fig. 5. One half of each prepared weld was mapped using a grid of approximately 140 Vickers indents. The opposite half of each prepared weld was mapped using the Rockwell C test method. The hardness map did not span the entire plate thickness, because the tensile sample gauge could only be isolated from the center region of the plate. In fact, the map extended into the wall 0.09 in. (2.3 mm) from both the inner and outer machined plate surfaces, as this distance is the average difference between the gauge and shank radii, or half the difference in diameters: $(D_S - D_G)/2$ — Fig. 5. It is clear in Fig. 5 that the tensile bar specified by NACE TM0177 and the chosen weld geometry did not allow for isolation of actual weld cap regions in the gauge sections.

Table 2 — Welding Parameters and Hardness Mapping Results

Weld Condition	Relative Peak Hardness	Voltage (Volts)	Current (Amps)	Travel Speed (in./min)	Energy Input (kJ/in.)	Preheat (°F)	Hardness Range (HV 10-kg)	Peak Hardness (HV 10-kg)	Peak Hardness (HRC)	Peak HV Converted to HRC
X70 Condition I	High	23	172	15.7	15.1	Room Temp.	189–295	295	<20	29.1
X70 Condition II	Medium	23	172	15.7	15.1	250	185–269	269	<20	25.3
X70 Condition III	Low	33	300	14.6	40.7	250	154–236	236	<20	19.8
X80 Condition I	High	23	172	15.7	15.1	Room Temp.	190–293	293	20.2	28.8
X80 Condition II	Medium	23	172	15.7	15.1	250	199–286	286	<20	27.8
X80 Condition III	Low	33	300	14.6	40.7	250	179–247	247	<20	21.8

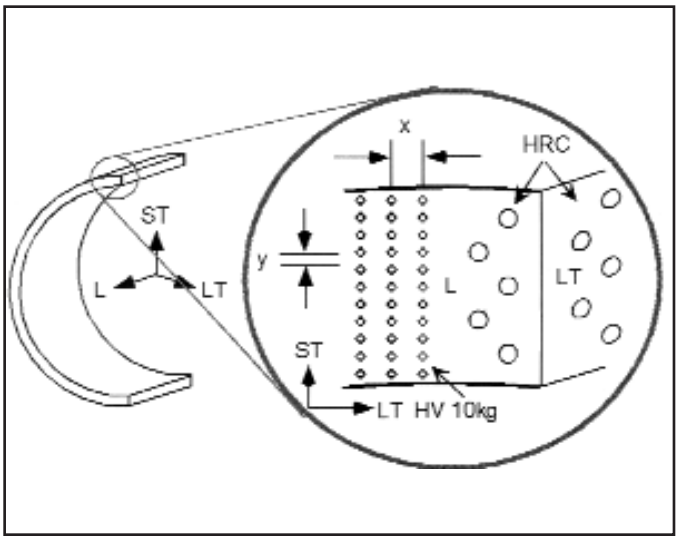

Fig. 3 — Schematic of through-wall hardness measurements.

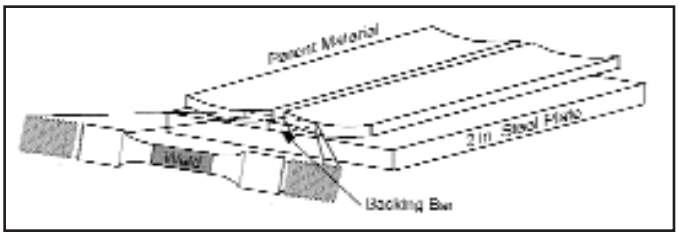

Fig. 4 — Schematic of setup for welding of plates to simulate girth welds.

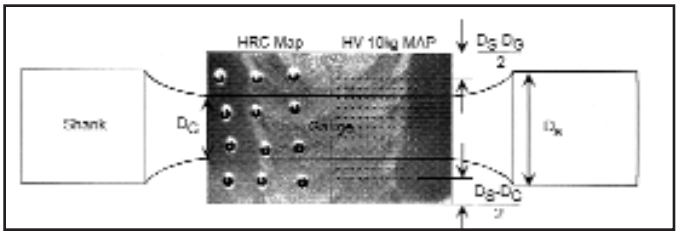

Fig. 5 — Macrograph of indents from hardness mapping overlaid by schematic of tensile sample shown at proper magnification relative to the weld.

A test matrix was employed to examine the effects of weld hardness, applied stress, and H_2S concentration on the SSC performance of the X70 and X80 welded samples. The three weld conditions produced a range in specimen peak weld hardness. Two applied stresses, 80% and 100% of the specified minimum base yield, were used in the test matrix. These high stresses were applied in order to duplicate the high residual tensile stresses encountered in non-postweld-heat-treated in-service weldments (Ref. 11). The NACE TM0177-A solution (Ref. 5) was used as a base solution: 5.0 wt-% NaCl + 0.5 wt-% glacial acetic acid in deionized H_2O. A range in H_2S concentration was achieved by bubbling the solution with 100%, 30%, or 10% H_2S (balance N_2) gas mixtures. The use of 100% H_2S exactly reproduced the standard test method, but the H_2S-N_2 mixtures created a major modification. The H_2S testing was performed in a special lab at CC Technologies. Proving rings were used for static load application and nitrogen was used for solution deaeration. All testing procedures outlined in NACE TM0177 were followed, except for the fact that diluted H_2S gas mixtures were used for several testing schedules.

After specimen removal, each specimen was examined optically at 10X in order to reveal any apparent surface cracking, as per the NACE TM0177-A standard. Cracking observed at 10X was sectioned and metallographically prepared to determine if SSC was the cause. In addition to the NACE failure criterion, a more detailed cracking investigation was performed. Even samples that passed the NACE criteria were examined for internal flaws. Details of the failure investigation procedure and results are given elsewhere (Ref. 7).

Results

Figure 6 displays the Rockwell C hardness results for the L and LT sections of each base material. The HV 10-kg measurements were converted to equivalent HRC values, and are included in Fig. 6 for comparison (X70 L CONV and X80 L CONV). The X80 converted HV measurements indicate that HRC 22 was exceeded in both the inner and outer peak-hardness bands. Actual HRC test results show that neither material exceeded the HRC 22 threshold. In fact, the X70 measurements were well below HRC 20, which is the lower limit for reporting HRC values. The highest Rockwell reading in the X80 material was HRC 22. Comparison between the actual HRC readings and the converted Vickers hardness reveals that the HV technique slightly overestimates hardness, even where there is not a steep hardness gradient, such as in the middle of the plate. However, there is no way to determine which hardness scale provides the more accurate readings. The HRC measurements may very well underestimate hardness in this case. In general, due to the indentation size produced in each hardness scale, Vickers hardness is able to detect localized hard spots and HRC hardness provides an average reading of the tested area.

The multipass welding employed for the welds created complex HAZ subregions that have been discussed in the literature (Ref. 12). These HAZ regions include the coarse-grained HAZ (CGHAZ), the grain-refined HAZ (GRHAZ), the intercritical HAZ (ICHAZ), the subcritical HAZ (SCHAZ),

the intercritically reheated coarse-grained HAZ (IRCG) and the subcritically reheated coarse-grained HAZ (SRCG). The latter regions were investigated at higher magnification to characterize the transformations that occurred. Figure 7 displays micrographs from the CGHAZ regions of both the X70 and X80 Condition I final welds. The Condition I weld produced the hardest overall weld microstructures, which were located in the CGHAZ. The X70 CGHAZ contained upper bainite (ferrite sideplates + interplate carbides) and lower bainite (carbides within ferrite plates), whereas the X80 CGHAZ contained only upper bainite. The ferrite portion of the upper bainite adopted a Widmanstätten "basket weave" that nucleated at a preferred orientation relative to the prior austenite grain boundaries (Kurdjumov-Sachs relationship) (Ref. 13). The CGHAZ grain size was very large relative to the base material grain size and exhibited large variability with position in each weld. Figure 8 displays the CGHAZ regions in the X70 and X80 Condition III welds, which had considerably higher heat inputs (40 kJ/in. vs. 15.1 kJ/in.) and a high weld preheat (250°F) that produced substantially lower CGHAZ cooling rates. The lower cooling rates produced a coarser ferrite side plate structure. The GRHAZ (not shown) in both alloys was characterized by grain refinement compared to the original base grain size. However, the X70 ICHAZ was evidenced by the "fuzzy pearlite" microstructure — Fig. 9. The intercritical HAZ (ICHAZ) in the X80 was virtually indistinguishable from the adjacent GRHAZ. Figure 10 displays the intercritically reheated coarse-grained HAZ (IRCG) microstructure encountered in both X70 and X80 multipass welds. Austenite islands nucleated in the CGHAZ grain boundaries, and also in the grain interiors during reheating from an overlay weld pass (Ref. 14). Upon cooling, the austenite islands can transform into twinned martensite (Ref. 14).

A hardness map of the X70 Condition I sample appears in Fig. 11. The peak hardness measured in the X70 Condition I weld was 295 HV. Relatively high hardness regions were encountered deep within the weldment. The hardness data generated from the six hardness maps is summarized in Table 2. There is a general reduction in peak sample hardness from Condition I to Condition III in both materials, indicating that the change in welding parameters had the desired effect. Peak HV 10-kg hardness measurements were located in the CGHAZ, close to the fusion boundary, in all welds. It was difficult to accurately center HRC measurements on the CGHAZ due to the indent size and sample manipulation. The Vick-

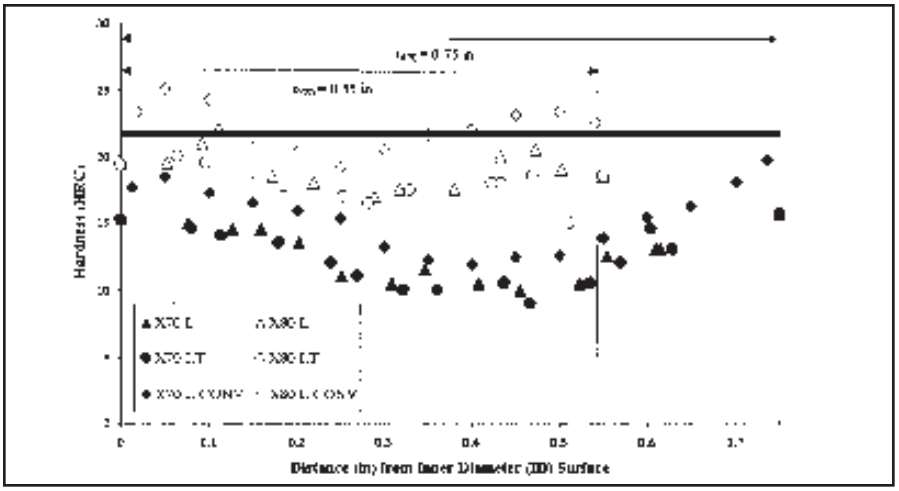

Fig. 6 — Base material through-wall hardness traverses. L and LT indicate traverses in the longitudinal and long transverse sections, respectively. L CONV indicates HV 10-kg data from the longitudinal section converted to the HRC scale.

Table 3 — Welding Conditions

Process:	Automated GMAW
Welding Wire:	ER70S-3 (S: Solid Wire, 3: Med Silicon, 0.045 in.)
Shielding Gas:	75Ar-25CO_2
Contact-Tip-to-Work Distance:	¾ in.

Table 4 — Condition I Final Weld Hardness (HV 10-kg) in Cap and Tensile Sample

	X70	X80
Cap Range	299–336	284–295
Weld Peak	336	295
Sample Peak	295	293

Table 5 — Results of SSC Test Matrix

	X70 High Hardness (Peak 310 HV 10-kg)		X80 High Hardness (Peak 293 HV 10-kg)	
Condition I	80% Yield	100% Yield	80% Yield	100% Yield
10% H_2S	FN HAZ	DEF HAZ	FI (Base Metal)	P
30% H_2S	FN HAZ	FN HAZ	DEF (Base Metal)	P
100% H_2S	FN HAZ	FI HAZ	FN HAZ	DEF HAZ
	X70 Medium Hardness (Peak 269 HV 10-kg)		**X80 Medium Hardness (Peak 286 HV 10-kg)**	
Condition II	80% Yield	100% Yield	80% Yield	100% Yield
10% H_2S	FI (Base Metal)	FI (Base Metal)	P	FI (Base Metal)
30% H_2S	P	P	FI (Base Metal)	DEF HAZ
100% H_2S	FI WM	DEF WM	DEF HAZ	DEF HAZ
	X70 Low Hardness (Peak 236 HV 10-kg)		**X80 Low Hardness (Peak 247 HV 10-kg)**	
Condition III	80% Yield	100% Yield	80% Yield	100% Yield
10% H_2S	P	FI HAZ	P	DEF HAZ
30% H_2S	P	FI HAZ	FI (Base Metal)	DEF HAZ
100% H_2S	P	FN WM	P	DEF HAZ

Key: FN – NACE Failure; FI – Internal Failure (passed NACE criteria); P – Pass; DEF – Double-Ended Fracture.

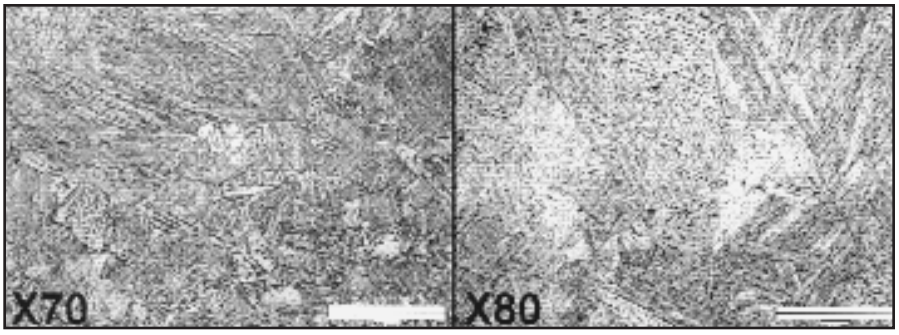

Fig. 7 — Microstructure of CGHAZ for Condition I welds of X70 (left) and X80 (right).

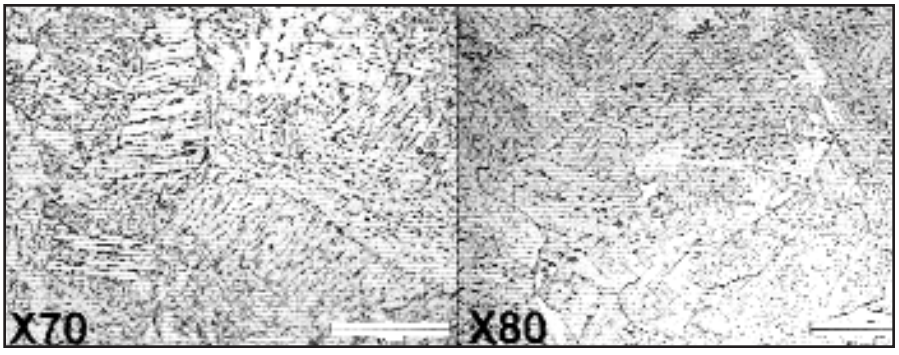

Fig. 8 — Microstructure of CGHAZ for Condition III welds of X70 (left) and X80 (right).

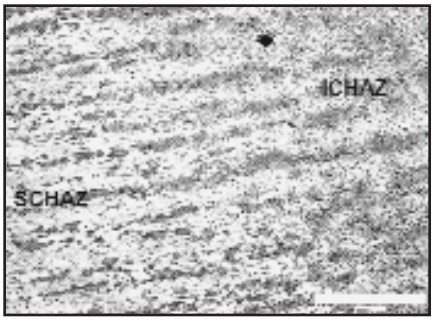

Fig 9 — Interface between SCHAZ and ICHAZ in X70.

ers testing equipment was equipped for accurate placement of indents within thousandths of an inch. The HRC test equipment did not have these capabilities, and difficulty sampling specific regions was further increased due to optical parallax and poor sample lighting.

The HRC hardness values are substantially lower than the converted Vickers data, especially when comparing the hardness values obtained in or around the CGHAZ from either method. In fact, no HRC weld measurement exceeded HRC 22, while measurements exceeding HV 248 (equivalent to HRC 22) were numerous in the Condition I and II weldments in both materials. Table 2 demonstrates that the conversions of the peak Vickers measurements to equivalent HRC values could not be reproduced with the Rockwell C test method. For example, the X70 Condition I results indicate a peak weld hardness of 29.1 HRC when converted from the Vickers measurement (295 HV), but the actual peak HRC measurement was below the reportable limits of the HRC test method (<20 HRC).

As described above, the hardest regions in the final cap weld regions could not be isolated in the reduced-diameter tensile gauge section due to geometric constraints. Peak weld hardness measurements were performed on the X70 and X80 Condition I full-weld cross sections in order to determine the peak weld (as opposed to sample) hardness. The testing focused on the CGHAZ in the untempered cap passes. The Condition II and III welds were not tested, because the Condition II weld cap passes employed a different preheat (RT) than the underlying passes (250°F) in order to minimize tempering, and the Condition III welds did not contain cap passes. The peak weld measurements were then compared to peak sample hardness values (determined by the weld hardness maps), as shown in Table 4. The underlying X80 Condition I welds were not tempered significantly, as the hardness difference between the peak cap hardness and the peak sample hardness is only 2 HV. However, the X70 underlying weld passes were tempered significantly when compared to the peak cap hardness. This tempering effect may have a significant influence on extrapolation of the SSC testing results to allowable in-service cap weld hardness.

Vickers hardness measurements in each respective weld region were tabulated from inspection of the hardness maps. The mean hardness values for each weld region in both the X70 and X80 welds are given in Figs. 12 and 13, respectively. The X80 Condition III (Fig. 13) weld exhibits considerable softening in the ICHAZ and IRCG regions such that measured hardness values were lower than the minimum base metal hardness. A significantly lower strength can be expected in these regions. This softening has been reported in the HAZ of TMCP steels (Ref. 15). While the Condition III welding parameters produced a relatively soft ICHAZ and SCHAZ microstructures in the X70 material, these regions remained within the base metal hardness range.

The results of the sulfide stress cracking tests are given in Table 5. The failures are distinguished in Table 5 according to the nature of the failure. NACE failures were observed at 10X, and complete double-ended fractures (DEF) or samples that experienced complete separation are denoted. The crack initiation region is denoted for each DEF. Internal failures were found solely by either scanning electron microscope (SEM) investigation or metallographic cross-sectioning. Base metal failures are distinguished from the typical weld metal (WM) or heat-affected zone (HAZ) failures. Repeat tests were performed on each weld condition at 100% YS and 100% H_2S, and are discussed elsewhere (Ref. 7).

The SSC testing revealed that the X70 Condition I welds were not suitable for sour service, failing even when exposed to lower H_2S concentrations, despite being below HRC 22. The peak HRC hardness values for all welds were below HRC 22, and the peak HV 10-kg values are included for each weld condition in Table 5. Post-exposure hardness testing around an internal crack indicated that the X70 I welds contained higher hardness than determined with the hardness mapping (310 HV vs. 295 HV). Ignoring the base metal failures (since the high applied stresses were meant to duplicate weld residual stress), the X70 II, X80 I, and X80 II welds exhibited SSC resistance at lower H_2S concentrations despite their high hardness (> 248 HV). Surprisingly, the soft X80 III welds were highly susceptible to complete, double-ended SSC fracture. The X70 and X80 Condition III welds failed at 100% YS, at all concentrations of H_2S. The applied stress seemed to dictate SSC resistance in the Condition III welds, as these welds were resistant at 80% YS. Metallographic examination and SEM fractography indicated that brittle SSC crack propagation was typically associated with the CGHAZ and IRCG in the double-ended

fractures. The base metal failures in the X70 were associated with the centerline segregation region (CSR). In some samples, SSC was observed in the CSR if and when it intersected the sample surface. An example of cracks formed at the intersection of the CSR with the surface is given in Fig. 14A. Internal SSC cracking was also observed if the CSR intersected the ICHAZ, rather than emerging on the sample surface — Fig. 14B. The X70 III welds failed in this manner.

Discussion

NACE MR0175 requires that carbon steels and their weldments utilized in sour service conditions not exceed HRC 22 (Ref. 1), thereby placing importance on the predictive capabilities of the Rockwell C test method. However, HSLA weld hardness testing is typically performed using the Vickers hardness measurement technique (Refs. 16, 17) because of the difficulty of measuring narrow HAZ regions in low heat input welds. The relatively large HRC indenter senses an average of the hardness of a narrow heat-affected zone (Ref. 18). This difference in size between the Vickers and HRC indents is portrayed accurately in the X70 Condition I hardness map in Fig. 11. The inability of the HRC test method to test narrow HAZ regions is evidenced by the disparity between the HRC and Vickers testing results produced by this study. The HRC weld measurements were consistently lower than converted Vickers measurements. This difference was also exhibited in the base metal hardness traverses. However, there was a systematic difference between the measured base metal HRC values and the converted HV values. The converted HV values overestimated the measured HRC values by about 2–3 HRC points in the base metal. On the other hand, the difference between the converted HV weld measurements and the HRC weld measurements varied by as much as 9 HRC points (X80 I, Table 2). This deviation cannot be attributed to the error in the hardness conversion equation alone. Rather, it implicates the averaging effect of the HRC indenter. Figure 15 shows individual Vickers hardness traverses from each X70 weld hardness map (Conditions I, II, and III). Very steep gradients in hardness are seen in the HAZ, especially in the Condition I weld. The X70 Condition I weld exhibited a change in hardness of about 60 HV over a distance of 0.03 in. This distance is comparable to the diameter of the HRC indent, which ranged from 0.034 to 0.038 in. in these materials. The same averaging effect was also found in the X80 welds. In short, the HRC technique does not have the appropriate hardness resolution required for characterizing low heat input weld HAZs.

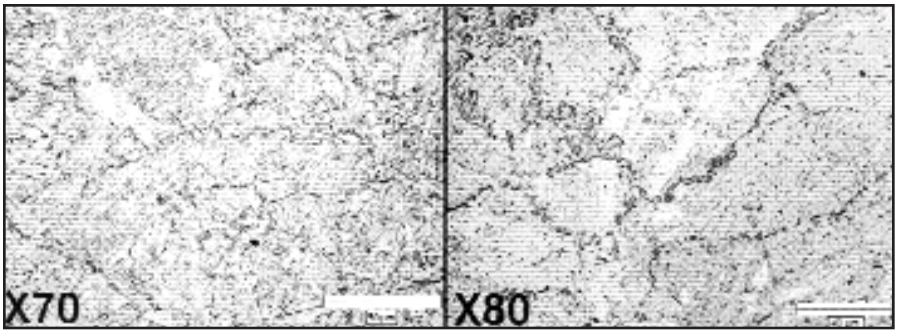

Fig. 10 — Intercritically reheated coarse-grained HAZ for X70 (left) and X80 (right).

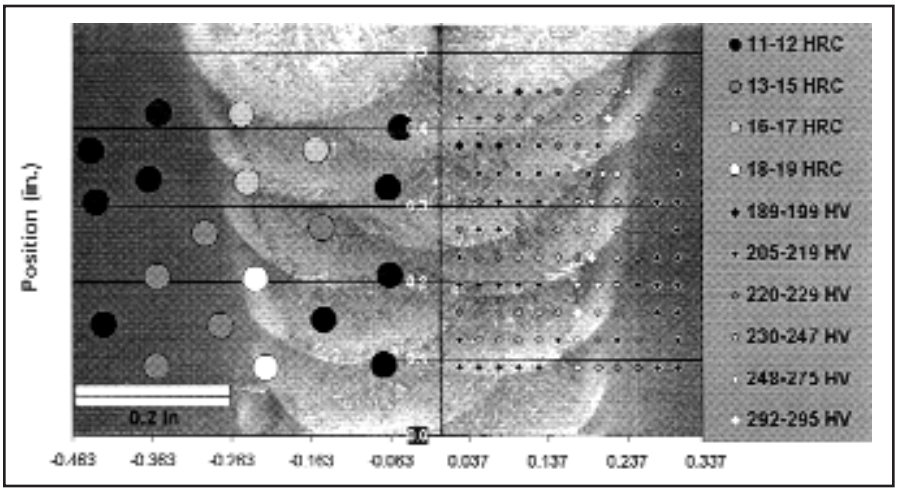

Fig. 11 — X70 Condition I hardness map. The symbols represent the locations of the indents, and the size of the symbols represents the approximate size of the indents. The hardness scale is given on the right.

The comparison between the HRC and HV test methods has strong implications on the conservatism of both the NACE MR0175 and BS4515 materials requirements when considering sour service welding applications. Because the HRC test method cannot accurately test narrow HAZ regions, the HRC requirement is not conservative when applied to low heat input welds. This view is based on the fact that hardness depends on the microstructure, which, in turn, reflects susceptibility to sulfide stress cracking (Ref. 19). If very hard regions (more susceptible) exist in a weldment that cannot be characterized with the HRC method, then any standard based on this measurement would not be conservative.

The results of the hardness testing in this work also have implications on the comparison between the NACE MR0175 requirements (<HRC 22) and the relaxation in weld hardness afforded by the BS4515 standard. As of July 1989, BS4515 has permitted weld cap hardness values up to 275 HV (HRC 26) (Ref. 20). This relaxation was based on work performed by Robinson on as-welded X60 pipe, in which he suggested that average hardness as high as 370 HV (HRC 38) was permissible under similar hydrogen absorption conditions without externally applied stress (Ref. 20). Later work by Walker led to further relaxation in the BS4515 requirement, allowing peak cap hardness of 300 HV (HRC 30) in outer cap regions in stressed pipes (Refs. 20, 21). However, caution should be exercised when applying Walker's HRC results, as these values were determined by conversion of measured HV values, not by direct measurement (Ref. 20). The HRC 22 limit was recommended for weld regions exposed directly to sour environments by both Robinson and Walker, and adopted by BS4515 (Refs. 20–22). However, this value was based on test results involving welds characterized only with the HV test method (Ref. 20). Hardness mapping in this work showed that welds containing hard regions on the order of 295 HV only registered peak HRC readings of 20–21. Presumably, welds with HV readings in excess of 300 HV would still only register HRC 22 or less, depending on the width of the HAZ. Therefore, there may not be a

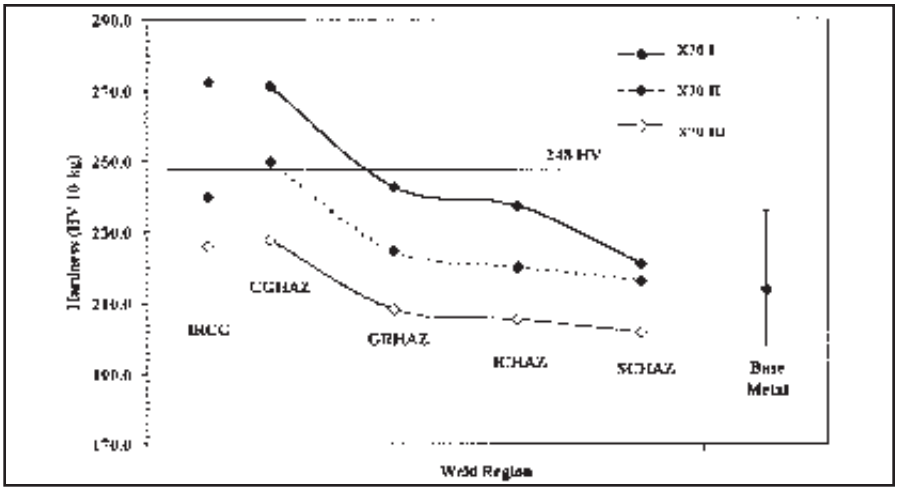

Fig. 12 — Mean hardness for different regions in X70 welds.

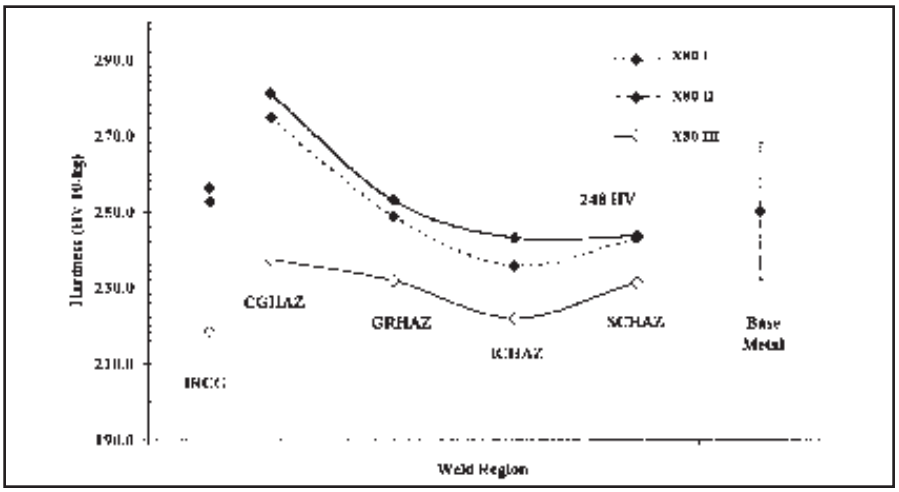

Fig. 13 — Mean hardness for different regions in X80 welds.

large difference between the NACE MR0175 and BS4515 standards when qualifying low heat input welds in HSLA materials.

The results of the SSC testing portion of this work and extrapolation to service are discussed in more detail elsewhere (Ref. 8). In general, the X70 welds (excluding base material failures) exhibited an increase in SSC susceptibility with increased weld peak hardness, as would be expected based on the long-standing correlation between hardness and SSC susceptibility (Ref. 1). The X70 I weld was produced without preheat and generated the highest hardness measurement (310 HV). The high hardness coarse-grained heat-affected zone (CGHAZ) was predominantly implicated in both complete fractures and terminal cracking. Generally, post-test hardness testing showed good agreement with the hardness mapping results other than the X70 I welds as discussed above and the X80 III welds as discussed below. The X70 II welds (15.1 kJ/in., 250°F), which contained hard regions exceeding 248 HV (HRC 22), failed in the standard TM0177 tests (100% H_2S) at both applied stresses, yet exhibited resistance with lower H_2S concentrations (10%, 30% H_2S). The failures that did occur in the X70 II welds were in the base metal and fusion zone. The X70 III welds (<248 HV) exhibited no susceptibility with the lower applied stress (80% YS), yet failed under the more aggressive testing conditions with the high applied stress (100% YS). The failures in the X70 III welds were either associated with weld inclusions or SSC at the IRCG/CSR interface. The X70 II and III welds were, to some degree, resistant to SSC, whereas the X70 I weld was determined not to be suitable for sour service, with a peak sample hardness of 310 HV (10kg).

The X80 welds exhibited very interesting trends when considering only those failures that occurred in welded regions (not base metal failures). Increasing hardness tended to increase resistance to SSC, especially at the applied stress equivalent to 100% of the specified minimum yield of the base material (80 ksi). The Condition I X80 weld exhibited good resistance to the modified NACE TM0177 testing conditions (10%, 30% H_2S). The Condition II weld was more susceptible under more severe testing conditions, and failed at 100% YS, 30% H_2S, where the Condition I weld did not. The X80 Condition III (Peak HV = 247 HV) weld exhibited poor performance at 100% YS. The applied stress level dominated the SSC susceptibility. The fact that susceptibility increased with lower hardness for the same applied stress and H_2S conditions suggests that the localized ICHAZ and IRCGHAZ softening may play a role in SSC susceptibility for the X80 welds.

Fracture analyses implicated not only the influence of the high-hardness CGHAZ on cracking and complete failure, but also the importance of the intercritically reheated heat-affected zone (IRCG) and, in the X70 samples, the ICHAZ/CSR intersection. The deleterious effect of the CGHAZ, ICHAZ, and IRCGHAZ regions on SSC performance has been reported by several investigators. One property shared by each of these regions is that they all have shown the potential to contain martensite-austenite (MA) constituent (Refs. 14, 23, 24). The volume-fraction of MA constituent has been linked to a lack of toughness (Ref. 10). Not only is the MA constituent brittle itself, it creates stress concentrations in the surrounding matrix (Ref. 14). Double thermal cycling of the CGHAZ during multipass welding creates the IRCG. The CGHAZ and IRCGHAZ weld regions were implicated either in crack initiation or propagation in most of the welds tested. The upper bainite CGHAZ is recognized as a low toughness microstructure (Refs. 12, 24). Heat treatment has not been shown to improve the low toughness of this region (Ref. 24). The CGHAZ and IRCG zones may be susceptible to SSC cracking due to MA constituent, which can comprise the carbide phase in upper bainite (CGHAZ) or decorate the prior austenite grain boundaries in the IRCG (Refs. 12, 23). MA constituent has been shown to reduce toughness of the ICHAZ substantially (Ref. 24), and promote inter- and transgranular cracking (depending on location) (Ref. 24).

In the X80 Condition III welds, the IRCG zone was particularly susceptible to crack initiation and propagation, especially at applied stresses of 80 ksi. The X70 Condition III weld did not exhibit this same high susceptibility to either complete fracture or terminal cracking, despite the use of the same welding parameters (40 kJ/in., 250°F preheat). The X80 III

IRCG and ICHAZ were softened considerably when compared to the base metal — Fig. 13. It is reasonable to assume that, due to the localized softening, strain localization occurred predominantly in these softened zones during loading. Therefore, plasticity was introduced into the X80 III samples and possibly the X80 II samples. This preferential straining in softened weld regions is mentioned by Pargeter and Gooch, who attributed SSC cracking in the ICHAZ of a welded TMCP steel to this phenomenon (Ref. 19). Localized deformation in this region may also account for the higher post-test HV hardness values in the X80 III IRCG relative to the as-welded values reported in the hardness maps. In the X70 welds, SSC susceptibly decreased with lower hardness and the same degree of softening exhibited in the X80 III welds was not observed in the IRCG and ICHAZ regions. The mean hardness values of these regions in all weld conditions were within the base metal hardness range. High heat input welds are not recommended for these types of steels, but were used in this study in order to examine the effect of low weld hardness.

Presumably, the X70 Condition I weld is more susceptible to SSC than the X80 I weld because of its higher carbon content (0.16 vs. 0.029 wt-%). Higher carbon equivalents and higher carbon content are directly related to higher hardness and the amount of MA constituent (Ref. 10). It has been established that extra-low-carbon steels are more resistant to SSC in as-welded conditions, due to the absence of highly susceptible martensite (Ref. 25). The higher manganese and low sulfur would promote higher hardenability of CGHAZ and IRCG in the X80, so the low phosphorus and carbon content in each alloy probably dominates the toughness response (Refs. 10, 19, 26, 27). Mn and S segregate in the grain boundaries, the former promoting the formation of martensite and the latter promoting ferrite formation. The effect of austenite island (MA precursor) hardenability on ICHAZ toughness was shown by Fairchild et al. (Ref. 12).

The X80 Condition I weld HAZ was much more resistant to SSC than the X70 Condition I HAZ, especially considering the values of the absolute stresses impressed on this region in the respective alloys. Failures were focused in the CGHAZ and IRCG in these conditions. The thermomechanical history of the alloy is essentially erased in the CGHAZ due to the high austenizing temperatures and the CGHAZ is typically the hardest (strongest) weld region, so the base metal yield strength means little in this weld region. The IRCG results from reheating of the CGHAZ, so its microstructure is independent of thermomechanical history of the alloy. The X80 Condition I CGHAZ/IRCG was resistant to SSC (at lower H_2S concentrations) at applied stresses equivalent to 80 ksi (100% base YS), while the X70 failed under similar conditions at applied stresses of 57 ksi (80% base YS). This may be a result of the deleterious effects that increasing carbon content has on weld performance. Normally, comparison of steel susceptibility to SSC based on absolute stresses is not meaningful. On the other hand, as the strength of the steel (UTS) increases, the susceptibility to SSC is expected to increase.

Alternatively, low carbon martensite formation (on a larger scale than in the MA constituent) in the X70 CGHAZ may have produced the high susceptibility to cracking observed in the X70 I Condition. The presence of martensite was not confirmed with optical or SEM methods. However, the tempering response observed in this weld region upon comparison of the peak cap CGHAZ hardness to underlying CGHAZ hardness values may suggest the formation of low carbon martensite. Further characterization would be required to affirm its presence.

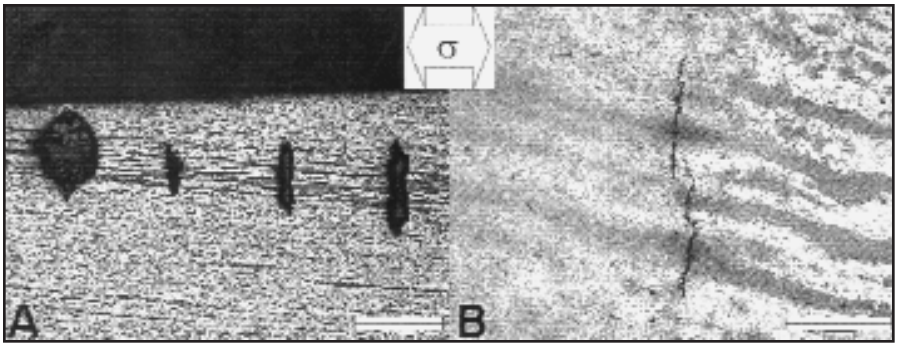

Fig. 14 — Sulfide stress cracks associated with the center segregated region (CSR). The arrows show the stress orientation. A — Surface cracks; B — internal cracks associated with the ICHAZ.

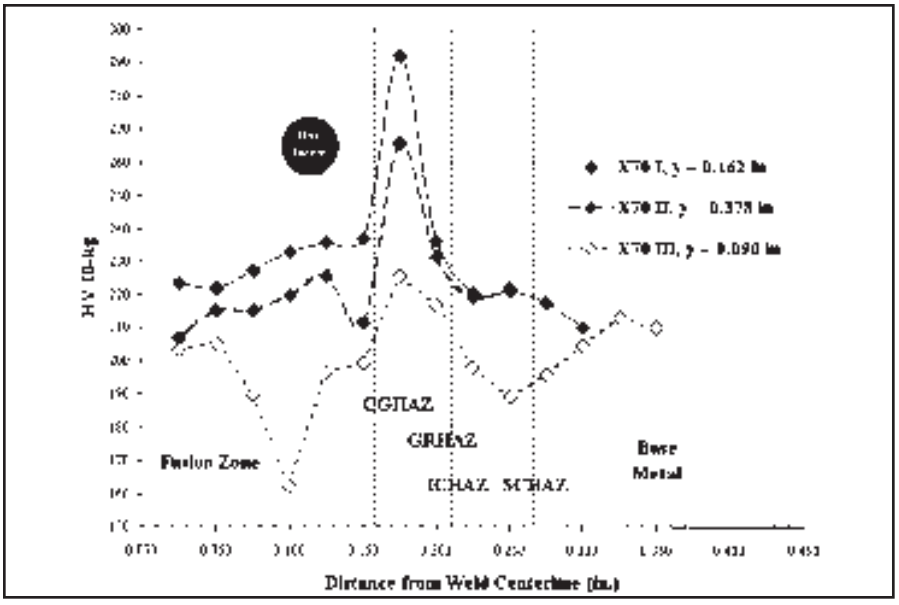

Fig. 15 — HV 10-kg hardness traverses for welds in X70 with different weld conditions.

Conclusions

- The Rockwell C hardness test method does not accurately characterize hardness in narrow heat-affected zones (HAZ) due to an averaging effect produced by the large indenter size.
- The HRC 22 threshold hardness is a nonconservative criterion for weldments in sour service carbon steels because of averaging effects in narrow HAZ regions.
- The HV 10-kg technique is recommended for characterizing peak weld hardness with the low heat input welds investigated in this study (~15 kJ/in.), and is warranted as an alternative to the Rockwell C method on carbon steel welds in conjunction with the NACE MR0175 requirements.
- A maximum hardness of 248 HV should be maintained for carbon steel

base materials and regions of carbon steel weldments that are in direct contact with sour service environments.

• The Rockwell C method did not reproduce the high HAZ hardness values measured using the HV 10-kg technique in narrow heat-affected zones. Therefore, the relaxation in allowable hardness afforded by BS 4515 should only be used in context with the appropriate Vickers measurements, as the relaxation recommendation was based on testing of welds characterized using actual HV measurements, not actual HRC measurements.

• The martensite-austenite (MA) microconstituent that has been attributed to low HAZ toughness contributed to low SSC resistance in the HAZ.

• The low-carbon (~0.03 wt-% C) X80 steel was subject to HAZ softening relative to the base metal, which increased SSC susceptibility due to strain localization. A minimum HAZ hardness may be justified for these types of steels.

• The low-carbon (~0.03 wt-% C) X80 steel was more resistant to SSC in the as-welded condition and tolerated much higher absolute tensile stresses than the as-welded X70. In general, based on experimental observations (Table 5), X80 pipe steel was more resistant in Condition I than X70. However, X70 steel was more resistant in Condition III than X80.

• SSC experiments showed that the centerline segregated region (CSR) in control rolled steels is susceptible to SSC, and may dictate both alloy and weld susceptibility.

• The NACE failure criteria were not adequate for detecting internal SSC cracking associated with the CSR/weld intersection. A more detailed metallographic evaluation is recommended for carbon steel weldments in which the base metal contains a CSR. Otherwise, the NACE criteria were adequate for detecting weldment failures.

Acknowledgments

This project was funded by Edison Welding Institute Cooperative Research Program 43564-IRP. We would like to acknowledge personal contributions from Charlie Ribardo (formerly at EWI) and Gary Todd (CC Technologies). CC Technologies donated the use of its laboratory facility for H_2S testing performed in this study.

References

1. MR0175 materials requirement standard: *Sulfide Stress Cracking Resistant Metallic Materials for Oilfield Equipment*. Houston, Tex.: NACE.

2. Berkowitz, B. J., and Heubaum, F. H. 1984. The role of hydrogen in sulfide stress cracking of low alloy steels. *Corrosion* 40(5): 240–245.

3. Kane, R. D. 1985. Roles of H_2S in behaviour of engineering alloys. *Int. Met. Rev.* 30(6): 291–301.

4. Turn, J. C., Wilde, B. E., and Troianos, C. A. 1983. On the sulfide stress cracking of line pipe steels. *Corrosion* 39 (9): 364–370.

5. TM0175 *Test Method Standard: Laboratory Testing of Metals for Resistance to Specific Forms of Environmental Cracking in H_2S Environments* 1996. Houston, Tex.: NACE.

6. Walker, R. A. 1989. The significance of local hard zones on the outside of pipeline girth welds. Final contract report. PR-164-804. Cambridge, U.K.: The Welding Institute.

7. Omweg, G. 2001. Sulfide stress cracking resistance of welded high-strength low-alloy steels. MS thesis. Columbus, Ohio: The Ohio State University.

8. Omweg, G., Frankel, G., Bruce, W., and Koch, G. 2001. The performance of welded high-strength low-alloy steels in sour environments. Accepted for publication in *Corrosion*.

9. Cayard, M. S., and Kane, R. D. 1997. Large-scale wet hydrogen sulfide cracking performance: evaluation of metallurgical, mechanical, and welding variables. *Corrosion* 53(3): 227–233.

10. Morrison, W. B. 1990. Status of microalloyed steel development. *The Metallurgy, Welding, and Qualification of Microalloyed (HSLA) Steel Weldments*. Eds. J. T. Hickey, D. G. Howden, and M. D. Randall. Miami, Fla.: American Welding Society. pp. 3–33.

11. 1990. Sulfide stress cracking resistance of pipeline welds. Proposed technical committee report draft. Houston, Tex.: NACE.

12. Fairchild, D. P., Bangaru, N. V., Koo, J. Y., Harrison, P. L., and Ozekcin, A. 1991. A study concerning intercritical HAZ microstructure and toughness in HSLA steels. *Welding Journal* 7012: 321-s to 329-s.

13. Shewmon, P. G. 1969. Transformations in metals. *Materials Science and Engineering.* Ed. P. G. Shewmon. New York, N.Y.: McGraw-Hill.

14. Akselsen, O. M., Grong, O., and Solberg, J. K. 1987. Structure-property relationships in intercritical heat-affected zone of low-carbon microalloyed steels. *Materials Science and Technology* 3.

15. Shiga, C. 1990. Effects of steelmaking, alloying, and rolling variables on the HAZ structure in microalloyed plate and linepipe. *The Metallurgy, Welding, and Qualification of Microalloyed (HSLA) Steel Weldments.* Eds. J. T. Hickey, D. G. Howden, and M. D. Randall. Miami, Fla.: American Welding Society. pp. 327–350.

16. Harrison, P. L., and Hart, P. H. M. 1990. Influences of steel composition and welding procedure on the HAZ toughness of thick section structural steels. *The Metallurgy, Welding, and Qualification of Microalloyed (HSLA) Steel Weldments.* Eds. J. T. Hickey, D. G. Howden, and M. D. Randall. Miami, Fla.: American Welding Society. p. 818.

17. McHaney, J. H., Bruno, T. V., Craig, B. D., and Brownlee, J. K. 1995. Fundamentals of materials and welding for sour service pipelines. *The Internal Corrosion and Pipe Protection Conference Proceedings.* Pipeline and Gas Journal and Systems Integrity. pp. 123-161.

18. 1993. Draft guidance notes on hardness testing of components and weld zones for sour service. *Draft Guidance Notes.* EFC.

19. Pargeter, R. J., and Gooch, T. G. 1994. Welding for sour service. *Materials, Maintenance and Inspection in the Oil and Gas Industry.* The Welding Institute.

20. Walker, R. A., Ginn, B. J., Pargeter, R. J., Gooch, T. G., and Noble, D. N. 1993. The significance of local hard zones on the outsides of pipes. *8th Symposium on Line Pipe Research.* The Welding Institute.

21. Unknown. 1991. TWI study relaxes hardness limits. *Materials Performance* (April): pp. 55.

22. Robinson, J. L. 1981. A preliminary assessment of the risk of hydrogen cracking in service of external welds on vessels with sour contents. LD22532, TWI.

23. Davis, C. L., and King, J. E. 1993. Effect of cooling rate on the intercritically reheated microstructure and toughness in high strength low alloy steel. *Materials Science and Technology* 90.

24. Thaulow, C., Paauw, A. J., and Guttormsen, K. 1987. The heat-affected zone toughness of low-carbon microalloyed steels. *Welding Journal 66(9)*: 266-s to 279-s.

25. Onsqien, M. I., Akselsen, O. M., Grong, O., and Kvaale, P. E. 1990. Prediction of cracking resistance in steel weldments. *Welding Journal* 69(1): 45–51.

26. Asahi, H., Sogo, Y., Ueno, M., and Higashiyama, H. 1989. Metallurgical factors controlling SSC resistance of high-strength, low-alloy steels. *Corrosion* 45(6): 519-527.

27. Graville, B. A. 1990. Hydrogen cracking sensitivity of HSLA steels. *The Metallurgy, Welding, and Qualification of Microalloyed (HSLA) Steel Weldments.* Eds. J. T. Hickey, D. G. Howden, and M. D. Randall. Miami, Fla.: American Welding Society.pp.127–150.